文章编号：1001－9014(2019)04－0439－06

DOI:10.11972/j.issn.1001－9014.2019.04.008

Design of multi-gain-stage avalanche photodiodes with low excess noise

TANG Yan*, LI Bin, CHEN Wei, HUANG Xiao-Feng, CHAI Song-Gang, ZHAO Kai-Mei, ZHANG Cheng, GAO Xin-Jiang

(The 44th Institute, China Electronics Technology Group Corporation, Chongqing 400060, China)

Abstract: On the basis of deadspace multiplication theory(DSMT) numeric model and modified deadspace multiplication theory(MDSMT) model, the excess noise of multi-gain-stage avalanche photodiodes with different multiplication stage and different carrier initial energy was analyzed. The effects on excess noise of different width of impact-ionization multiplication layer, electron-heating layer and different doping of electric field control layer were also studied. At the same time, the results obtained from DSMT model were compared with the results from Van Vliet model and McIntyre model. By adjusting the width of impact-ionization multiplication layer, electron-heating layer and the doping of electric field control layer, a structure relatively optimizing was acquired by DSMT numeric simulation. The excess noise was comparable to the result of Van Vliet model at $k_s = 0.057$.

Key words: excess noise, multi-gain-stages, deadspace multiplication theory(DSMT), deadspace

PACS: 85.60.Gz, 73.40.Kp, 81.15.Hi

低过剩噪声级联倍增雪崩探测器设计

唐 艳*, 李 彬, 陈 伟, 黄晓峰, 柴松刚, 赵开梅, 张 承, 高新江

(中国电子科技集团公司第四十四研究所,重庆 400060)

摘要:基于弛豫空间倍增理论数值模型和修正的弛豫空间倍增理论模型,分析了不同倍增级数和不同载流子初始能量时级联倍增雪崩探测器的过剩噪声.研究了不同碰撞离化倍增层厚度、不同电子预加热层厚度、不同电场控制层掺杂浓度对过剩噪声因子的影响.同时,比较了DSMT模型、Van Vilet模型和McIntyre模型得到的结果.通过调整碰撞离化倍增层厚度、电子预加热层厚度和电场控制层掺杂浓度,DSMT数值模拟获得了一个相对优化的结构,其过剩噪声与Van Vliet模型 $k_s = 0.057$ 时相当.

关 键 词:过剩噪声;级联倍增;弛豫空间倍增理论(DSMT理论);弛豫空间

中图分类号:O471 **文献标识码**:A

Introduction

Avalanche gain of APD results from impact ionization with stochastic nature, thus the gain is random and the randomness is characterized by the excess noise. In 1966, McIntyre derived excess noise factor formula to evaluate the excess noise.[1] However, this formula cannot calculate the excess noise of APDs with thin multiplication layers less than 400 nm, because it doesnot take the deadspace effect into consideration. Soon afterward, Hayat *et al.* established dead-space multiplication theory (DSMT) numeric models to analyze the excess noise of a single-carrier injection double-carrier multiplication APDs with thin multiplication layers. The results from this theory fit the experiment results well.[2] It makes up the shortage of McIntyre formula.

Although the excess noise of APDs with thin multiplication layers are lower, an unwanted result exists that the mean gain will also be lowered because longer impact ionization chains have been eliminated. The problem can be effectively solved by APD's multi-gain-stage design in which high gain and low excess noise can be obtained at the same time.[3] The same as quantum cascade detector (QCD), multi-gain-stage APDs also use energy band engineering. Institute of Semicondutors, Chinese Academy of Sciences reported GaAs quantum cascade infrared photodetector which obtain low noise and dark current.[4]

Received date: 2018-12-10, **revised date**: 2019-06-03 **收稿日期**:2018-12-10, **修回日期**:2019-06-03

Foundation items: Joint Equipment Prophecy Fund (6141B08110301)

Biography: TANG Yan(1985-), female, Shandong, China. Master. Research fields focus on InP-based photodiodes.

* **Corresponding author**: E-mail: liuxuchitang@163.com

The difference is that multi-gain-stage APDs use impact ionization engineering to obtain high gain in addition to low noise.

This paper analyzes the effect on excess noise and mean gain of multi-gain-stage APDs with different width of multiplication layer and electron-heating layer and different dopings of electric field control layer, and a 10-gain-stage design is achieved with ideal excess noise and gain.

1 DSMT theory

Impact ionization can occur when the electrons and holes possess sufficient kinetic energy. The minimum distance that a newly generated carrier must travel in order to build up enough energy to become capable of initiating ionization is called dead space. The effect of dead space on the excess noise and mean gain is determined by using a recurrence method.

For an electron, it travels in the opposite direction of electric field and ionize and form two electrons and a hole after a random distance. Similarly, a hole travels in the direction of electric field and ionize and form an electron and two holes after a random distance. Electrons and holes repeat this process until they reach the edge of the multiplication layer. The parameters in the DSMT numeric models are as follows.

1.1 dead space

The expression for dead space is as follows:

$$q\int_{x}^{x+d_e(x)} \varepsilon(y)\,\mathrm{d}y = E_{ie}(x + d_e(x)) \quad , \quad (1)$$

$$q\int_{x-d_h(x)}^{x} \varepsilon(y)\,\mathrm{d}y = E_{ih}(x - d_h(x)) \quad , \quad (2)$$

where $\varepsilon(x)$ is electric field at x location, $E_{ie}(x)$ and $E_{ih}(x)$ are impact ionization threshold energy of electrons and holes at location x respectively, $d_e(x)$ and $d_h(x)$ denote the dead space of electrons and holes at location x respectively, q is the electronic charge.

1.2 Probability density function (PDF) of distance to impact ionization

After a random distance an impact ionization occurs.[5] $h(\xi|x)$ is the probability density function of the impact ionization of electrons and holes that locate at x and move to location ξ and impact ionize at location ξ, impact ionization can only occur when the motion distance ξ is larger than the dead space of carriers at location x. PDF is given by,

$$h_e(\xi \mid x) = \begin{cases} \alpha(\xi \mid x)\,\mathrm{e}^{-\int_{x+d_e(x)}^{\xi}\alpha(y|x)\,\mathrm{d}y}, & x + d_e(x) \leqslant \xi \leqslant \omega \\ 0, & 0 < \xi \leqslant x + d_e(x) \end{cases} \quad , \quad (3)$$

$$h_h(\xi \mid x) = \begin{cases} \beta(\xi \mid x)\,\mathrm{e}^{-\int_{\xi}^{x+d_h(x)}\beta(y|x)\,\mathrm{d}y}, & 0 \leqslant \xi \leqslant x - d_h(x) \\ 0, & x - d_h(x) \leqslant \xi \leqslant x \end{cases} \quad , \quad (4)$$

$\alpha(\xi|x)$ and $\beta(\xi|x)$ are impact ionization rates at location ξ of electrons and holes that come from location x without initial energy respectively, that are calculated by,

$$\alpha(x)/\beta(x) = A \cdot \exp\left[-\left(\frac{B}{E(x)}\right)^{m}\right] . \quad (5)$$

1.3 The recurrence equations of gain and excess noise

For double-carrier-multiplication avalanche photodiodes, $Z(x)$ is used to denote the random number of all electrons and holes progeny produced by an electron at location x and itself. Similarly, $Y(x)$ is used to denote the random number of all electrons and holes progeny produced by a hole at location x and itself. Assume the range of multiplication layer is from 0 to w, and electrons moves along direction of positive x, holes moves along opposite direction. The random gain generated by only an electron injecting is $[Z(0) + Y(0)]/2$, clearly $Y(0) = 1$, so the random gain is $[Z(0) + 1]/2$. The recurrence equations are as follows.[4]

$$z(x) = \langle Z(x) \rangle = \left[1 - \int_{x}^{W} h_e(\xi \mid x)\,\mathrm{d}\xi\right] + \int_{x}^{W} [2z(\xi) + y(\xi)]\, h_e(\xi \mid x)\,\mathrm{d}\xi \quad , \quad (6)$$

$$y(x) = \langle Y(x) \rangle = \left[1 - \int_{0}^{x} h_h(\xi \mid x)\,\mathrm{d}\xi\right] + \int_{0}^{x} [2y(\xi) + z(\xi)]\, h_h(\xi \mid x)\,\mathrm{d}\xi \quad , \quad (7)$$

$$z_2(x) = \langle Z^2(x) \rangle = \left[1 - \int_{x}^{W} h_e(\xi \mid x)\,\mathrm{d}\xi\right] + \int_{x}^{W} [2z_2(\xi) + y_2(\xi) + 4z(\xi)y(\xi) + 2z^2(\xi)]h_e(\xi \mid x)\,\mathrm{d}\xi \quad , \quad (8)$$

$$y_2(x) = \langle Y^2(x) \rangle = \left[1 - \int_{0}^{x} h_h(\xi \mid x)\,\mathrm{d}\xi\right] + \int_{0}^{x} [2y_2(\xi) + z_2(\xi) + 4y(\xi)z(\xi) + 2y^2(\xi)]h_h(\xi \mid x)\,\mathrm{d}\xi \quad . \quad (9)$$

Original values of $z(x)$, $z_2(x)$, $y(x)$ and $y_2(x)$ at boundaries are $z(0) = 1$, $z_2(0) = 1$, $y(w) = 1$ and $y_2(w) = 1$, original values at other locations are zero.

After getting steady solutions from the recurrence equations, the mean gain and excess noise can be calculated.

$$\mathrm{GDSMT} = \frac{1 + z(0)}{2} \quad , \quad (10)$$

$$\mathrm{FDSMT} = \frac{z_2(0) + 2z(0) + 1}{(z(0) + 1)^2} \quad . \quad (11)$$

2 The modified DSMT theory (MDSMT)

Different from DSMT theory, the modified DSMT theory considers that the carriers gained initial energy when they go through non-zero electric field region before entering multiplication layer, thus the energy needed to obtain from the multiplication layer for the first impact ionization is reduced.[2]

If the injecting carrier's initial energy is $E0$, then the initial dead space d_{e0} is given by:

$$q\int_{x}^{x+d_{e0}(x)} \varepsilon(y)\,\mathrm{d}y = E_{ie}(x + d_{e0}(x)) - E0 \quad . \quad (12)$$

Clearly, if the carrier's initial energy before entering the multiplication layer is larger than the ionization threshold energy in the boundary of multiplication layer, then $d_{e0} = 0$.

In addition, the pdf of the distance to the first impact ionization for the injecting carrier is:

$$h_{e0}(\xi) = \begin{cases} \alpha(\xi)\mathrm{e}^{-\int_{d_{e0}(x)}^{\xi}\alpha(y)\mathrm{d}y}, & d_{e0}(x) \leqslant \xi \leqslant \omega \\ 0, & 0 < \xi \leqslant d_{e0}(x) \end{cases} . \quad (13)$$

$Z_0(x)$ is used to denote the random number of all electrons and holes progeny produced by an electron at location x and itself. The probability density function of the first impact ionization is $h_{e0}(\xi)$. The following formula can be obtained.

$$z_0(x) = < Z_0(x) > = [1 - \int_x^W h_{e0}(\xi)\mathrm{d}\xi] + \int_x^W [2z(\xi) + y(\xi)]h_{e0}(\xi \mid x)\mathrm{d}\xi , \quad (14)$$

$$z_{20}(x) = < Z_0^2(x) > = \left[1 - \int_x^W h_{e0}(\xi)\mathrm{d}\xi\right] + \int_x^W [2z_2(\xi) + y_2(\xi) + 4z(\xi)y(\xi) + 2z^2(\xi)]h_{e0}(\xi \mid x)\mathrm{d}\xi . \quad (15)$$

Putting the steady solutions from the DSMT theory recurrence equations into the above two equations, the mean gain and excess noise can be calculated, the results are as follows.

$$\mathrm{CMDSMT} = \frac{1 + z_0(0)}{2} , \quad (16)$$

$$\mathrm{FMDSMT} = \frac{z_{20}(0) + 2z_0(0) + 1}{(z_0(0) + 1)^2} . \quad (17)$$

3 Van Vliet theory

If the ionization multiplication processes including two types of carriers, in low gain, it must consider the discrete nature of the ionization process for both carriers. The excess noise value from Van Vliet is lower than that from McIntyre formula in sufficiently low gain.[6] In multi-gain-stage APD including both hole-ionization and electron-ionization, the excess noise is given by:

$$F(M_{\mathrm{DC}}, k_s, P_e) = 1 + \frac{(1 - \frac{1}{M_{\mathrm{DC}}})(1 - k_s)}{2 + P_e(1 - k_s)} \cdot \left[- P_e + 2\frac{(1 - k_s P_e^2)}{(1 + k_s P_e)}(M_{\mathrm{DC}} k_s \frac{(1 + P_e)}{(1 - k_s)} + \frac{1}{1 + P_e}) \right] , \quad (18)$$

where P_e is the electron-ionization probability per gain stage, J is the number of gain stages, k_s is the ratio of the hole-ionization probability per gain stage to P_e. The mean gain is given by:

$$M_{\mathrm{DC}}(J) = \frac{(1 + P_e)^J(1 - k_s)}{(1 + P_e k_s)^{J+1} - k_s(1 + P_e)^{J+1}} . \quad (19)$$

4 Multi-gain-stage single photon avalanche photodiode

Multi-gain-stage single photon avalanche photodiodes adjust the doping concentration to change the electric field profile in the multiplying junction, thus further control the carrier's energy by accelerating it in high electric field region and releasing its energy in the forms like phonon scattering. The impact ionization threshold energy is changed by adjusting the alloy composition in multi-gain-stage single photon avalanche photodiodes.

The randomness of multiplication process can be reduced by means of suppressing the hole-ionization and enhancing electron-ionization, meanwhile spatially localizing the latter.

The structure of multi-gain-stage single photon APD is designed as Fig. 1. Electrons can be pre-heated before injecting into impact ionization layer and holes can be injected cold by modulating the electric field profile. The low-field carrier relaxation regions in which holes and electrons lose their accumulated energy by random phonon scattering are used to separate the gain stages. Thus, the holes injected cold cannot impact ionize. Compared to two-carrier ionizations, ionizations only including electron-ionization decrease the number of impact ionization chains, furthermore narrow the gain distribution. Therefor, the multi-gain-stage single photon avalanche photodiodes suppress the excess noise.

The material of high-field multiplication layers in this structure is $Al_{0.336}In_{0.523}Ga_{0.141}As$, which lattice match with $In_{0.52}Al_{0.48}As$ and $In_{0.53}Ga_{0.47}As$ and is composed of 70% $In_{0.52}Al_{0.48}As$ and 30% $In_{0.53}Ga_{0.47}As$.

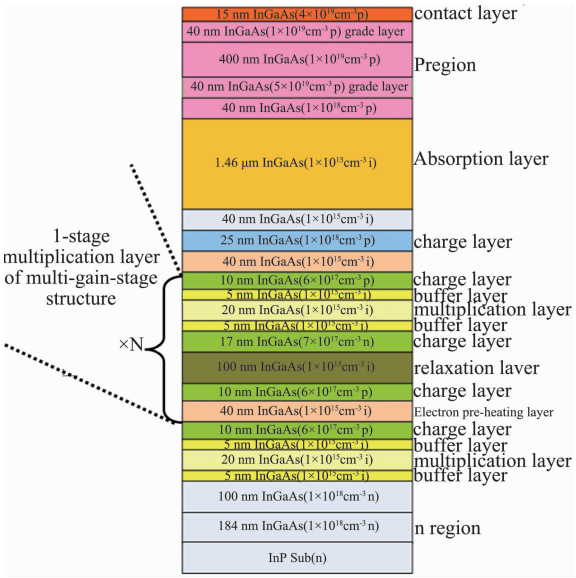

Fig. 1　Epitaxial layer structure of an multi-gain-stage single photon avalanche photodiode

图 1　级联倍增结光电探测器外延结构

The impact ionization threshold energies energy of electrons and holes in different materials are shown as Tabel 1[7-9] where E_{ie} are threshold energies of electrons and E_{ih} are threshold energies of holes.

Tabel 1　Threshold energies

表 1　能量阈值

	E_{ie}/eV	E_{ih}/eV
$In_{0.53}Ga_{0.47}As$	1.2	1
$In_{0.52}Al_{0.48}As$	2.15	2.3
$Al_{0.336}In_{0.523}Ga_{0.141}As$	1.865	1.91

The material parameters A, B and m to calculated the impact ionization rates in the Eq. 5 are shown in Table 2.[7-9] The results are obtained by fitting the experimental values of ionization coefficients to the model given by Eq. 5.

Table 2 Material parameters A、B、m
表 2 材料参数 A、B、m

		A/cm^{-1}	B/V·cm^{-1}	m
$In_{0.53}Ga_{0.47}As$	α	1.8e7	1.95e6	1
	β	2.56e7	2.2e6	1
$In_{0.52}Al_{0.48}As$	α	4.17e6	2.09e6	1.20
	β	2.65e6	2.79e6	1.07
$Al_{0.336}In_{0.523}Ga_{0.141}As$	α	9.58e6	2.28e6	0.98
	β	1.02e7	2.46e6	0.96

5 Results and discussion

In the process of calculating dead space and ionization rates, the effect of phonon scattering is taken into consideration, that is the energy of a carrier which is reseted to zero after travelling a certain distance.[2,5,10] In addition, the effect on ionization rates results from the bandedge discontinuity of multilayer structures is ignored.[11] The results below are obtained in the photodiodes with each gain stage the same as the structure in Fig. 1 unless otherwise specified.

Figure 2 shows the electric filed of multiplication layers and the dead space distribution of a 10-stage APD at an average gain of $M=690$. Figure 3 plots the non-localized ionization rates and the scattering-aware ionization rates for electrons and holes. Taking phonon scattering in the energy relaxation layers into consideration centralizes the ionization events, electrons can ionize immediately upon entering the high field multiplication layers, meanwhile, the holes ionization rates decrease in each gain stage.

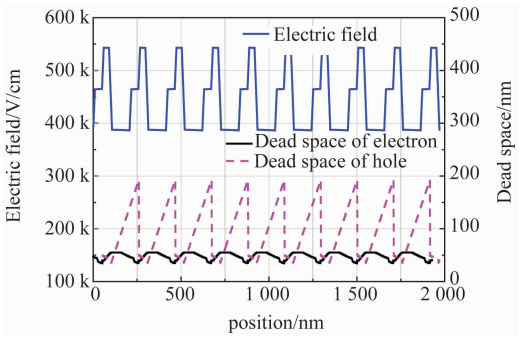

Fig. 2 The electric field and deadspace profile of multiplication layer in a 10-gain-stage APD ($M=690$)
图 2 10 级级联倍增 APD($M=690$)电场和弛豫空间分布

The excess noise factors are calculated theoretically for 3-gain-stage, 7-gain-stage and 10-gain-stage APD using DSMT theory, as shown in Fig. 4. The result of conventional InAlAs APD with 200 nm multiplication width is calculated for comparison. The results show that the excess noise factor of gain stage APD is better than that of conventional APD and the excess noise factor can be reduced significantly by increasing the number of gain stages.

The effects on excess noise of different width of high field multiplication layer and electrons pre-heating layer, doping concentration of charge layer are analyzed and compared, the results are shown in Figs. 5-7 respectively.

Figure 5 shows the excess noise predicted by the DSMT numeric model for a 10-stage APD with the width of high field multiplication layer at 10 nm, 15 nm and 35 nm respectively. The numeric results show that the excess noise firstly decreases and then increases with the decreasing of the width of multiplication layer, for example, the excess noise of APD with width at 10 nm is lager than that at 15 nm. In addition, if the multiplication layer is too narrow, the maximum gain can be suppressed.

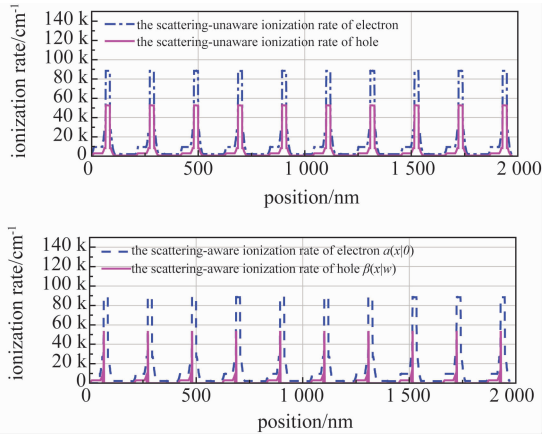

Fig. 3 Ionization rates (scattering-aware and no scattering-aware)
图 3 离化率(考虑声子散射和未考虑声子散射)

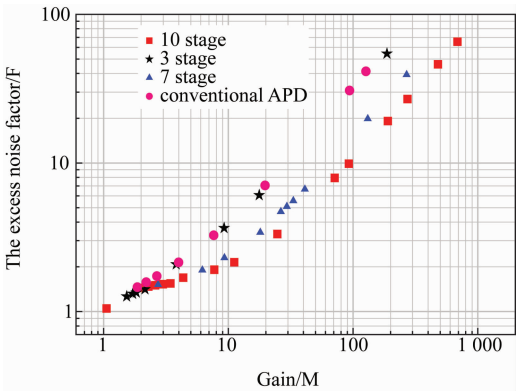

Fig. 4 The excess noise factor in 3-gain-stage, 7-gain-stage, 10-gain-stage APD and conventional InAlAs APD
图 4 3 级、7 级和 10 级级联 APD 和常规 APD 过剩噪声因子

Figure 6 shows the DSMT numeric model results of excess noise factor for a 10-stage, 20 nm-width multiplication layer APD with the width of electron pre-heating layer at 0 nm, 40 nm and 100nm respectively. Clearly,

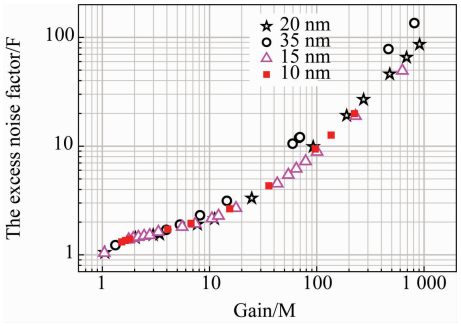

Fig. 5　The excess noise factor of structure with the width of multiplication layer at 10 nm, 15 nm, 20 nm and 35 nm
图 5　倍增层厚度分别为 10 nm,15 nm,20 nm 和 35 nm 时过剩噪声因子

the excess noise is larger when the width of electron pre-heating layer is larger at lower gain, the reason is that the dead space of electrons and holes are large in this condition. While the effect of the width of electrons pre-heating layer on the excess noise is small, because the electron dead space is small, in this condition the maximum gain is affected, such as decreasing the width of electron pre-heating layer to zero, the maximum gain is lower than 70.

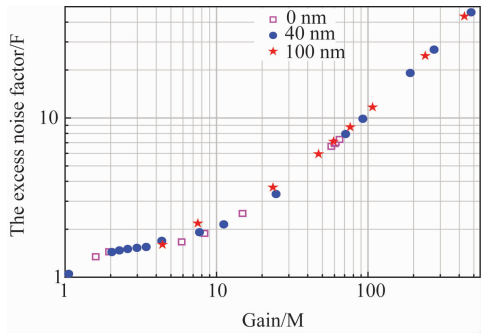

Fig. 6　The excess noise factor of structures with width of pre-heating layer at 0 nm, 40 nm and 100 nm
图 6　预加热层厚度分别为 0 nm,40 nm 和 100 nm 时过剩噪声因子

Figure 7 compares the excess noise of two 10-stage structures, one gain stage of one structure is as Fig. 1, the other's single gain stage is modulating the doping of three charge layer in Figs. 1 to 7E17 cm^{-3},7E17 cm^{-3}, 8.2E17 cm^{-3} and to 5E17 cm^{-3},5E17 cm^{-3},5.85E17 cm^{-3}. It is obvious that the excess noise factor and the maximum gain are affected.

Figure 8 shows the MDSMT theoretical numeric results of excess noise of a 10-stage cascaded multiplier APD with carrier initial energy of 0, 0.2 times and 1 times of threshold energy, respectively. The excess noise will reduce when the initial energy is taken into consideration, because the initial energy furthermore localize the carriers impact ionization.

Figure 9 shows the results from DSMT numeric model, McIntyre model formula and Van Vliet model formula. DSMT numeric result of a 10-gain-stage APD is approximately in accordance with results from McIntyre formula at $k = 0.086$ and $M > 100$. Furthermore, it is in accordance with the results of a 10-stage cascaded multiplier APD from Van Vliet formula at $k = 0.086$.

By modulating the width of multiplication layer of

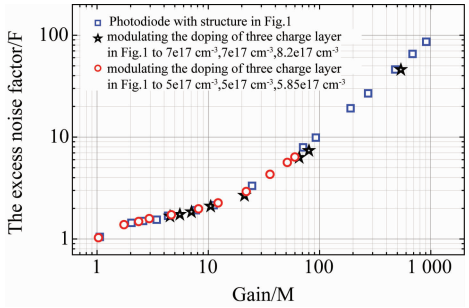

Fig. 7　The excess noise factor of different doping of charge layer(10-stage)
图 7　电荷层不同掺杂浓度时过剩噪声因子(10 级)

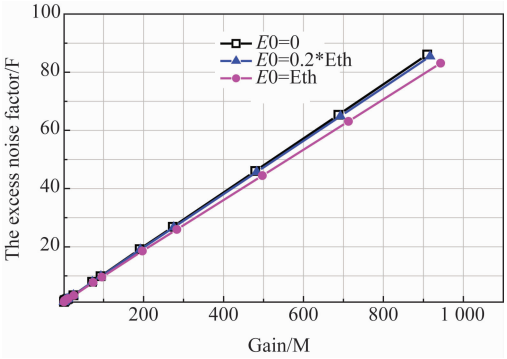

Fig. 8　The excess noise factor with the initial energy of 0, 0.2*E*th and *E*th
图 8　载流子初始能量为 0,0.2*E*th 和 *E*th 时的过剩噪声因子

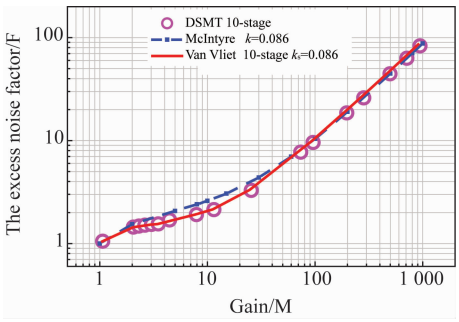

Fig. 9　Results from DSMT numeric theory(10-stage), Van Vliet model(10-stage, $k_s = 0.086$) and McIntyre model($k = 0.086$)
图 9　DSMT 数值理论模型(10 级),Van Vliet 模型(10 级,$k_s = 0.086$)和 McIntyre 模型($k = 0.086$)结果

Fig. 1 to 17 nm, the width of pre-heating layer to 30 nm, the doping of charge layer to 6E17cm^{-3}, 10E17cm^{-3}, 9.4E17cm^{-3}, a 10-stage cascaded multiplier APD is obtained, the excess noise factor of which is shown in Fig. 10. It is in accordance with the result from Van Vliet model at $k_s = 0.057$.

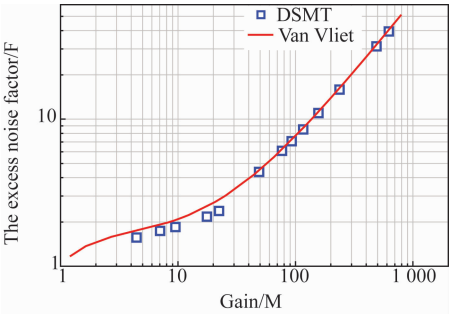

Fig. 10 Results of 10-stage DSMT (by modulating the structure in Fig. 1, the width of multiplication layer at 17 nm, the width of pre-heating layer at 30 nm, the doping of charge layer at 6E17cm^{-3}, 10E17cm^{-3}, 9.4E17cm^{-3}) and Van Vliet (10-stage, $k_s = 0.057$)

图 10 DSMT 10 级级联倍增模拟(模拟结构如图 1,倍增层厚度为 17 nm,预加热层厚度 30 nm,电场层掺杂浓度分别为 6E17cm^{-3},10E17cm^{-3},9.4E17cm^{-3})和 Van Vliet 模拟(10 级,$k_s = 0.057$)

6 Conclusions

The DSMT theoretical numeric results indicate the existence of better width values of high field multiplication layer and electron pre-heating layer and better doping values of charge layer to optimize the excess noise and multiplication gain. By modulating the structure parameters, a 10-stage cascaded multiplier APD is obtained, the excess noise factor of which is in accordance with the result from Van Vliet model at $k_s = 0.057$. DSMT theoretical numeric model can guide the structure design of the multi-gain-stage single photon photodiodes.

References

[1] McIntyre R J. Multiplication noise in uniform avalanche photodiodes [J]. *IEEE Trans. Electron Devices*, 1996, **13**(1):164 - 168.

[2] Hayat M M, Kwon O H, Wang S L, *et al*. Boundary effects on multiplication noise in thin heterostructure avalanche photodiodes: theory and experiment [J]. *IEEE Transactions Electron Devices*, 2002, **49**(12): 2114 - 2123.

[3] Williams G M, Ramirez D A, Hayat M M, *et al*. Time resolved gain and excess noise properties of InGaAs/InAlAs avalanche photodiodes with cascaded discrete gain layer multiplication regions [J]. *Journal of Applied Physics*, 2013, **113**(9): 093705-1-093705-11 .

[4] LIU Jun-Qi, ZHAI Shen-qiang, KONG Ning, *et al*. Quantum cascade infrared photodetectors [J]. *Infrared and Laser Engineering*(刘俊岐, 翟慎强, 孔宁, 等. 量子级联红外探测器, **红外与激光工程**), 2010, **40**(8):1397 - 1402.

[5] Hayat M M, Saleh B E A, Teich M C. Effect of dead space on gain and noise of double-carrier-multiplication avalanche photodiodes [J]. *IEEE Transactions Electron Devices*, 1992, **39**(3):546 - 552.

[6] Van Vliet K M, Friedmann A, Rucker L M. Theory of carrier multiplication and noise in avalanche devices-Part Ⅱ: Two-carrier processes [J]. *IEEE Transactions Electron Devices*, 1979, **ED-26**(5): 752 - 764.

[7] Saleh M A, Hayat M M, Kwon O H, *et al*. Breakdown voltage in thin Ⅲ-Ⅴ avalanche photodiodes [J]. *Applied Physics Letters*, 2001, **79**(24): 4037 - 4039.

[8] Saleh M A, Hayat M M, Saleh B E A, *et al*. Dead-space-based theory correctly predicts excess noise factor for thin GaAs and AlGaAs avalanche photodiodes [J]. *IEEE Transactions Electron Devices*, 2000, **47**(3): 625 - 633.

[9] Pearsall T P. Impact ionization rates for electrons and holes in Ga0.47In0.53As [J]. *Applied Physics Letters*, 1980, **36**(3):218 - 220.

[10] David J P R, Allma J, Adams A R, *et al*. Avalanche breakdown in $Al_xGa_{1-x}As$ alloys and Al0.3Ga0.7As/GaAs multilayers [J]. *Applied Physics Letters*, 1995, **66**(21): 2876 - 2878.

[11] Chia C K, David J P R, Plimmer S A, *et al*. Avalanche multiplication in submicron $Al_xGa_{1-x}As$/GaAs multilayer structure [J]. *Journal of Applied Physics*, 2000, **88**(5):2601 - 2608.